

Subthreshold antiproton production in pC, dC and α C reactions

H Müller¹, V I Komarov²

¹ Institut für Kern- und Hadronenphysik, Forschungszentrum Rossendorf,
Postfach 510119, D-01314 Dresden, Germany

² Joint Institute for Nuclear Research, LNP, 141980 Dubna, Russia

E-mail: H.Mueller@fz-rossendorf.de

Abstract. Data from KEK on subthreshold \bar{p} as well as on π^\pm and K^\pm production in pC, dC and α C reactions at energies between 3.5 and 12.0 A GeV are described for the first time within a unified approach. We use a model which considers a nuclear reaction as an incoherent sum over collisions of varying numbers of projectile and target nucleons. It samples complete events and thus allows for the simultaneous consideration of all final particles including the decay products of the nuclear residues. The enormous enhancement of the \bar{p} cross section, as well as the moderate increase of meson production in dC and α C compared to pC reactions, is well reproduced. In our approach, the observed enhancement near the production threshold is mainly due to the contributions from the interactions of few-nucleon groups.

PACS numbers: 24.10.-i, 24.10.Lx, 25.40.-h, 25.45.-z, 25.55.-e

1. Introduction

Subthreshold particle production in a nuclear reaction is understood as production below the energy threshold of the considered process in a free nucleon-nucleon (NN) collision. It is thus a nuclear phenomenon which may be explained by rather different assumptions on the properties of nuclear matter and on the interaction dynamics. Hereby, it is an open question to what extent subthreshold particle production is governed by properties of the nuclear ground state wave function and to what extent by the dynamical properties of nuclear matter, not reflected in the ground state description. The problem is far from a final solution at present and evidently requires a systematic study of high-momentum transfer processes, among them subthreshold particle production.

First measurements of subthreshold \bar{p} production in proton-nucleus collisions had been carried out [1–4] a few decades ago. Then investigations in nucleus-nucleus collisions [5–9] and more recent studies of proton-nucleus reactions [10] followed. In [11] for the first time light-ion-induced \bar{p} production has been investigated and an enormous enhancement of subthreshold \bar{p} production in deuteron-nucleus reactions compared to proton-nucleus interactions has been found. This fact has been confirmed by the final results of the KEK group [12]. They measured d- and α -induced reactions in the energy region between 2.5 and 5.0 GeV/nucleon and observed at

3.5 GeV/nucleon \bar{p} cross sections nearly two and three orders of magnitude larger than measured in proton-nucleus reactions.

Most of the descriptions proposed so far are based on transport calculations [13–22], thermodynamical considerations [23–26] or multi-particle interactions [27] and are devoted to proton and/or heavy-ion induced reactions. By measuring light-ion-induced subthreshold \bar{p} production the KEK group [12] intended to provide an experimental test for models in this transition region between proton and heavy-ion-induced reactions. To the best of our knowledge only one paper [19] has been published so far, which compares proton- and deuteron-induced \bar{p} production at subthreshold energies.

It should be stressed that all mentioned papers on subthreshold \bar{p} production consider the \bar{p} spectra without any relation to results concerning other reaction channels. At KEK [12], however, the spectra of π^\pm and K^\pm mesons were measured together with those of the antiprotons. In a recent paper [28], in the framework of the Rossendorf collision (ROC) model we simultaneously considered all these reaction channels for pC reactions and achieved a good reproduction of the data. In this paper, we extend these considerations to dC and αC reactions using the same parameter set.

In the ROC model, it is assumed that the nuclear residue becomes excited during the reaction due to the distortion of the nuclear structure by the separation of the participants from the spectators and due to the passage of the reaction products through the spectator system. In this way, final-state interactions are taken into account without making special assumptions concerning re-absorption, re-scattering, self-energies, potentials etc for each particle type (see also [28]). The fragmentation of the residual nuclei and the interaction of the nucleons participating in the scattering process are treated on the basis of analogous assumptions. Even more important, the phase-space of the complete final state consisting of the reaction products of the interaction of the participants as well as the fragments of the decay of the spectator systems is calculated. exactly This feature seems to be unique to the ROC model.

The plan of the paper is as follows. In section 2, the main ingredients of the ROC model are explained, which is used for the calculations to be presented. Section 3 contains a comparison of theoretical and experimental results for particle production with special emphasis on subthreshold \bar{p} production. A summary is given in section 4.

2. The model

The ROC model is implemented as a Monte Carlo generator which samples complete events for hadronic as well as nuclear reactions. It was successfully tested for pp interactions up to ISR energies in [29, 30], while nuclear reactions were considered in the papers [28, 31–34]. A detailed description of the model is given in [30] for the case of pp interactions and in a recent publication [28] for hadron-nucleus interactions. In the following the basic mathematics from the hadron-nucleus case [28] is extended to nucleus-nucleus reactions. Although in this paper we consider only light-ion-induced reactions, the given presentation is applicable to any nucleus-nucleus reaction. For the interested reader some minor changes in the ROC model relative to previous publications are indicated where appropriate.

The cross section of the interaction of two nuclei $(\mathcal{A}, \mathcal{Z}_A)$ and $(\mathcal{B}, \mathcal{Z}_B)$ characterized by their mass and charge numbers is considered as an incoherent sum over contributions from varying numbers a and b of nucleons (thereof z_a and z_b

protons) participating in the interaction

$$d\sigma(s) = \sum_{a=1}^{\mathcal{A}} \sum_{z_a=\max(0, a-\mathcal{N}_A)}^{\min(a, \mathcal{Z}_A)} \sum_{b=1}^{\mathcal{B}} \sum_{z_b=\max(0, b-\mathcal{N}_B)}^{\min(b, \mathcal{Z}_B)} \sigma_{az_a bz_b} \frac{dW(s; \alpha_{az_a bz_b})}{\sum \alpha_{az_a bz_b} \int dW(s; \alpha_{az_a bz_b})}. \quad (1)$$

Here, $s = P^2$ denotes the square of the centre-of-mass energy of the projectile-target system with $P = (E, \vec{P})$ being the total 4-momentum. The summation extends over all possible charge states ranging from clusters consisting completely of neutrons to those composed totally of protons. This range is restricted in cases where the number of available protons \mathcal{Z}_A (\mathcal{Z}_B) or neutrons $\mathcal{N}_A = \mathcal{A} - \mathcal{Z}_A$ ($\mathcal{N}_B = \mathcal{B} - \mathcal{Z}_B$) is smaller than the number of cluster nucleons. Expression $\sigma_{az_a bz_b}$ stands for the partial cross section of the interaction of clusters (a, z_a) with (b, z_b) , and the quantities $dW(s; \alpha_{az_a bz_b})$ describe the relative probabilities of the various final channels $\alpha_{az_a bz_b}$.

The partial cross sections $\sigma_{az_a bz_b}$ are calculated using a modified version of a Monte Carlo code [35] which is based on a probabilistic interpretation of the Glauber theory [36]. They account for sequential collisions between a projectile and b target nucleons capable of sharing their energy in close analogy with the virtual clusters of the cooperative model [37–44] (see [28] for a discussion of the novel features of the ROC model compared to the cooperative model). We use the profile function

$$\Gamma_{\mathcal{A}\mathcal{B}}(d) = \int \left[1 - \prod_{i=1}^{\mathcal{A}} \prod_{j=1}^{\mathcal{B}} (1 - p_{ij}) \right] \prod_{i=1}^{\mathcal{A}} \rho_{\mathcal{A}}(\vec{r}_i) d^3 r_i \prod_{j=1}^{\mathcal{B}} \rho_{\mathcal{B}}(\vec{r}_j) d^3 r_j$$

of the considered nuclei, which depends on the nucleon densities $\rho_{\mathcal{A}}(\vec{r}_i)$, $\rho_{\mathcal{B}}(\vec{r}_j)$ and the probability

$$p_{ij} = \exp(-d_{ij}^2 \pi / \sigma_{NN})$$

for an interaction of the i th projectile and the j th target nucleon with d_{ij} being the distance between the interacting particles. The nucleon density [45]

$$\rho_{\mathcal{A}}(\vec{r}) \propto (1 + \eta[1.5(f^2 - e^2)/f^2 + e^2 r^2/f^4]) \exp(-r^2/f^2) \quad (2)$$

of light nuclei $2 < \mathcal{A} < 20$ can be derived from a standard shell model wavefunction with $\eta = (\mathcal{A} - 4)/6$, $e^2 = f^2/(1 - 1/\mathcal{A})$ and $f = 1.55$ fm. For the deuteron the Paris deuteron wavefunction [46] is used. Then the NN cross section σ_{NN} is adapted such that the integral of the profile function over the impact parameter d reproduces the total inelastic $\mathcal{A}\mathcal{B}$ cross section

$$\sigma_{\mathcal{A}\mathcal{B}}^{in} = \int d^2 d \Gamma_{\mathcal{A}\mathcal{B}}(d).$$

The same calculation yields also the partial cross sections $\sigma_{az_a bz_b}$ we are interested in (for further details see [35]).

In (1), the quantities

$$dW(s; \alpha_{az_a bz_b}) \propto dL_n(s; \alpha_{az_a bz_b}) \rho_{\mathcal{A}}(\vec{P}_A) \rho_{\mathcal{B}}(\vec{P}_B) T^2 \quad (3)$$

describe the relative probabilities of the various final channels $\alpha_{az_a bz_b}$. They are given by the Lorentz-invariant phase-space factor $dL_n(s; \alpha_{az_a bz_b})$ multiplied by the square of the empirical reaction matrix element T^2 describing the collision dynamics. The Fermi motion is implemented via the momentum distributions of the residual nuclei $\rho_A(\vec{P}_A)$ and $\rho_B(\vec{P}_B)$, which are functions of the numbers a and b of participants. They are taken as Gaussians having, in case of nucleus \mathcal{A} , a width of

$$\sigma_a = \sqrt{aA/5/(A-1)} p_F \quad (4)$$

in accordance with the independent particle model [47] with $A = \mathcal{A} - a$ being the number of nucleons in the residue and p_F is the Fermi limit of the nucleus considered. For nucleus \mathcal{B} an analogous formula holds, and for the deuteron again the Paris deuteron wavefunction [46] is employed, now in momentum space. No special high-momentum component [48–53] is used in this paper.

The Lorentz-invariant phase-space is defined as the integral over the 3-momenta of the n primarily produced final particles with energy-momentum conservation taken into account

$$dL_n(s; \alpha_{az_a bz_b}) = \prod_{i=1}^n \frac{d^3 p_i}{2e_i} \delta^4(P - \sum_{i=1}^n p_i), \quad (5)$$

Here, the 4-momentum of the i th particle is denoted by $p_i = (e_i, \vec{p}_i)$ with $p_i^2 = m_i^2$.

For numerical calculations, the δ -function in equation (5) has to be removed by introducing a new set of $3n - 4$ variables to replace the $3n$ 3-momentum components. It is reasonable to choose a set of variables, which reflects the underlying physical picture of the interaction process. Using recursion [54] equation (3) can be rewritten in the form

$$dW(s; \alpha_{az_a bz_b}) \propto \frac{d^3 P_A}{2E_A} \rho_A(\vec{P}_A) \frac{d^3 P_B}{2E_B} \rho_B(\vec{P}_B) dW_A(M_A^2) dW_B(M_B^2) dW_C(M_C^2) \quad (6)$$

with the 4-momenta of the nuclear residues $P_A = (E_A, \vec{P}_A)$, $P_B = (E_B, \vec{P}_B)$ and of the participants

$$P_C = P - P_A - P_B = (E_C, \vec{P}_C), \quad (7)$$

the corresponding invariant masses are given by $M_A^2 = P_A^2$, $M_B^2 = P_B^2$ and $M_C^2 = P_C^2$. The integrals over the Fermi motion $d^3 P_A \rho_A(\vec{P}_A)/2E_A$ and $d^3 P_B \rho_B(\vec{P}_B)/2E_B$ separate, in accordance with the participant-spectator picture, the phase-spaces of the n_A and n_B nuclear fragments

$$dW_A(M_A^2) = dM_A^2 dL_{n_A}(M_A^2) T_A^2 \quad dW_B(M_B^2) = dM_B^2 dL_{n_B}(M_B^2) T_B^2 \quad (8)$$

from the phase-space

$$dW_C(M_C^2) = dL_{n_C}(M_C^2) T_C^2 \quad (9)$$

of the $n_C = n - n_A - n_B$ final particles arising from the participant system. In (8) and (9), the matrix element $T^2 = T_A^2 T_B^2 T_C^2$ is split into factors describing residue fragmentation (T_A^2 and T_B^2) and participant interaction (T_C^2). There is, however, a strong kinematic link between participants and spectators, since invariant mass M_C of the participant system, invariant masses M_A and M_B of the residues and the relative kinetic energy $\sqrt{s} - M_A - M_B - M_C$ of these three particle groups are connected by energy-momentum conservation. The excitation energy of the target residue comes usually into play via the spectral function (see e.g. [50]) derived from

electron scattering data. Unique to the ROC model, however, is the treatment of the spectator system in close analogy with the participant subsystem, since it calculates the complete final state of both the participants and the spectators.

The term $dW_C(M_C^2)$ in (6) and (9) describes the interaction of the groups of participating nucleons. Such a cluster-cluster reaction is treated in complete analogy to a hadronic reaction. In a first step intermediate particle groups called fireballs (FBs) are produced, which decay into so-called primary particles. The primary particles define the channels for which the weights (9) are calculated. Among them are resonances, which decay subsequently into stable hadrons. The dynamical input of the cluster-cluster reaction is implemented by the empirical transition matrix element

$$T_C^2 = T_i^2 T_{qs}^2 T_{ex}^2 T_t^2 T_1^2 T_{st}^2, \quad (10)$$

which describes the interaction process T_i^2 resulting in the production of $N \geq 2$ FBs, the production of hadrons T_{qs}^2 via the creation of quark-anti-quark ($q\bar{q}$) pairs, the invariant-mass distribution of the FBs T_{ex}^2 , the transverse T_t^2 and longitudinal T_1^2 momentum distribution of the FBs, and finally, some factors T_{st}^2 necessary for the calculation of the statistical weights. The interaction is assumed to proceed via colour exchange leading to the removal of valence quarks or of gluons from the interacting hadrons. Additional up, down and strange quark pairs are created in the ratio

$$u : d : s = 1 : 1 : \lambda_s \quad (11)$$

with $\lambda_s = 0.15$. They form the varying number of FBs, which subsequently decay into the final hadrons. The transverse momenta P_t of the FBs are restricted by an exponential damping (longitudinal phase-space) according to

$$T_t^2 = \prod_{I=1}^N \exp(-\gamma P_{t,I}) \quad (12)$$

with the mean $\bar{p}_t = 2/\gamma$. Two leading FBs, the remnants of the incoming clusters, get in the mean larger longitudinal momenta than the central FBs by weighting the events with

$$T_1^2 = (X_1 X_2)^\beta. \quad (13)$$

Here, the light-cone variables $X_1 = (E_1 + P_{z,1})/(e_a + p_{z,a})$ and $X_2 = (E_2 - P_{z,2})/(e_b - p_{z,b})$ are used with the 4-momenta of the participants given by $p_a = (e_a, \vec{p}_a)$ and $p_b = (e_b, \vec{p}_b)$. In [30], the high-energy approximations

$$X_1 = (E_1 + P_{z,1})/\sqrt{s} \quad \text{and} \quad X_2 = (E_2 - P_{z,2})/\sqrt{s}$$

were applied for the more symmetric pp interactions without any substantial influence on the results. For completeness, it should be mentioned that in the older publication [29] a transition matrix element with transverse damping only for the central FBs

$$T_t^2 = \prod_{I=3}^N \exp(-\gamma (P_{t,I})^2)$$

was applied while the 4-momenta t_{a1} and t_{b2} transferred to the leading FBs were restricted via

$$T_1^2 = \exp(\beta (t_{a1} + t_{b2})).$$

This variant worked well up to energies of about 50 GeV.

Each FB is characterized by two parameters, a temperature Θ_{FB} and a volume V_{FB} . The temperature determines the relative kinetic energy of the particles the FB decays into via

$$T_{ex}^2(\Theta_{FB}) = \prod_{I=1}^N (M_I/\Theta_{FB}) K_1(M_I/\Theta_{FB}), \quad (14)$$

while the volume defines the interaction region and influences mainly the particle multiplicity via the statistical factor $T_{st}^2 \propto V_{FB}^{n_C-1}$. In (14) K_1 stands for the modified Bessel function. Final hadrons are built-up by random recombination of the available quarks during the decay of the FBs. This procedure automatically ensures the conservation of all internal quantum numbers. Subsequently, resonances decay until the final state consisting of stable particles is reached. For a more detailed discussion of the hadronic matrix element the reader is referred to [30]. In this paper, we use the same set of parameters as in [30] for the description of the interaction of a single projectile nucleon with a single target nucleon. Most of the other terms in (1), however, contain clusters consisting of several nucleons. The basic parameters of the FBs emerging from such an interaction are fixed by scaling the volume and the temperature parameter according to

$$V_{FB} = V_{FB}^0 (a + b - 1) \quad \text{and} \quad \Theta_{FB} = \Theta_{FB}^{max} (a + b - 1)^{-1/3}. \quad (15)$$

It remains to consider the target residues, the structure of which is strongly disturbed by the interaction of the participants and subsequent final-state interactions. This leads to the excitation and decay of the spectator systems, which are characterized by the two parameters temperature Θ_R and volume V_R ($R = A$ or B in dependence on the residue under consideration) in the same way as the FBs emerging from the participant interaction. The part of the matrix element responsible for the residue fragmentation

$$T_R^2(\alpha_{az_a bz_b}^R) = T_{ex}^2(\Theta_R) T_{st}^2(\alpha_{az_a bz_b}^R) \quad R = A, B$$

is identical with the corresponding factors (10) applied to the hadronic FBs. In order to restrict the excitation energy transferred to the residue we use the asymptotic approximation of (14) for large mass and small temperature

$$T_{ex}^2(\Theta_R) = \sqrt{M_R/\Theta_R} \exp(-M_R/\Theta_R) \quad R = A, B. \quad (16)$$

An impact parameter dependence is assumed for the temperature parameter. This seems to be reasonable, because a peripheral collision with only few participating nucleons should excite the nuclear residue much less than a central collision with many participants. As a first guess we use

$$\Theta_A = \Theta_A^{max} [1 - \exp(-a/\bar{a}A^{1/3})] \quad \Theta_B = \Theta_B^{max} [1 - \exp(-b/\bar{a}B^{1/3})] \quad (17)$$

with \bar{a} as parameter, here fixed to $\bar{a} = 0.5$, which determines how fast the maximal temperatures Θ_A^{max} and Θ_B^{max} are reached with increasing number of participants. The value $\Theta_A^{max} = \Theta_B^{max} = 12$ MeV has been fixed in [28] from a comparison of the energy spectra of fragments from the reaction of 2.1 GeV protons with carbon measured at 90° [55] with ROC-model calculations.

All factors still necessary for a correct calculation of the relative weights of the various channels are collected in complete analogy with the corresponding factors for the FBs in the product of two terms with $R = A$ and $R = B$ according to

$$T_{st}^2(\alpha_{az_a bz_b}^R) = g(\alpha_{az_a bz_b}^R) \left(\frac{V_R}{(2\pi)^3} \right)^{n_R-1} \prod_{i=1}^{n_R} (2\sigma_i + 1) 2m_i. \quad (18)$$

It contains the spin degeneracy factors $(2\sigma_i + 1)$ and the volume V_R in which the particles are produced. The quantity $g(\alpha_{az_a bz_b}^R)$ is the degeneracy factor for groups of identical particles in the final state of the residue decay and prevents multiple counting of identical states. Further details of residue treatment can be found in [28].

3. Comparison with experimental data

In figure 1, the momentum spectra of π^\pm , K^\pm and \bar{p} from pC , dC and αC reactions measured at KEK [12] are displayed. The experimental efforts of the KEK group were motivated by measurements of large cross sections of subthreshold \bar{p} production in nucleus-nucleus reactions at LBL-BEVALAC [6, 7] and at GSI [8]. The authors [12] claimed that the use of light-ion beams for investigating subthreshold \bar{p} production should be useful to verify theoretical models. Secondary effects like re-scattering, re-absorption, self-energies, potentials etc., which hide and influence features of the primary production process, should be smaller than in heavy-ion reactions. Indeed, it is the outstanding feature of the data that in d- and α -induced reactions an enormous enhancement of \bar{p} production by nearly two and three orders of magnitude compared to p-induced interactions could be observed. The very fact of finding this enhancement in light-ion induced reactions makes this interaction type a candidate for the key to a deeper understanding of subthreshold \bar{p} production in nucleus-nucleus reactions.

The KEK group [12] interprets their \bar{p} data by using the ‘first-chance NN collision model’ from [48] where the internal nucleon momenta were extracted from backward proton production [49] as a superposition of two Gaussian distributions. In this way, the momentum spectra and the incidence-energy dependence of p-induced reactions could be successfully reproduced by adapting one normalization parameter. However, the application of this model to d-induced reactions using different deuteron wavefunctions and the normalization from p-induced interactions severely underestimates the \bar{p} cross sections at subthreshold energies. Thus, according to [12], the effect cannot be explained by the internal motion of the nucleons in the deuteron, even if a deuteron wavefunction with a high-momentum component is used.

In [19], \bar{p} production in $p+A$ and $d+A$ reactions is analysed within a phase-space model incorporating the self-energies of the baryons. It is claimed that the internal momentum distribution of the deuteron provides a natural explanation of the large enhancement under discussion.

To the best of our knowledge there is no paper which describes the further increase of subthreshold \bar{p} production in α -induced reactions. Thus, the approach presented here seems to be the first attempt to consider the whole set of projectiles in a unified picture. Beyond it, we also regard the whole set of ejectiles measured. This is of special importance since there is not only the enhancement of \bar{p} production, but also the increase of the K^- cross sections with increasing energy and mass number of the projectile around the elementary production threshold at 2.6 GeV. And also the completely different energy and projectile mass dependence of the pion production cross sections far above the threshold should be explained by a realistic approach.

In figure 1, the results of the ROC model calculated with one fixed parameter set are compared to the data [12]. The overall agreement is quite satisfactory in view of the different projectile types, the large region of incidence energies, the variety of ejectile species and the huge differences of many orders of magnitude in the considered cross section values. Particle yields are influenced by the suppression factor $\lambda_s = 0.15$ (equation (11)) of strange quarks and by the algorithm for creating the final hadrons

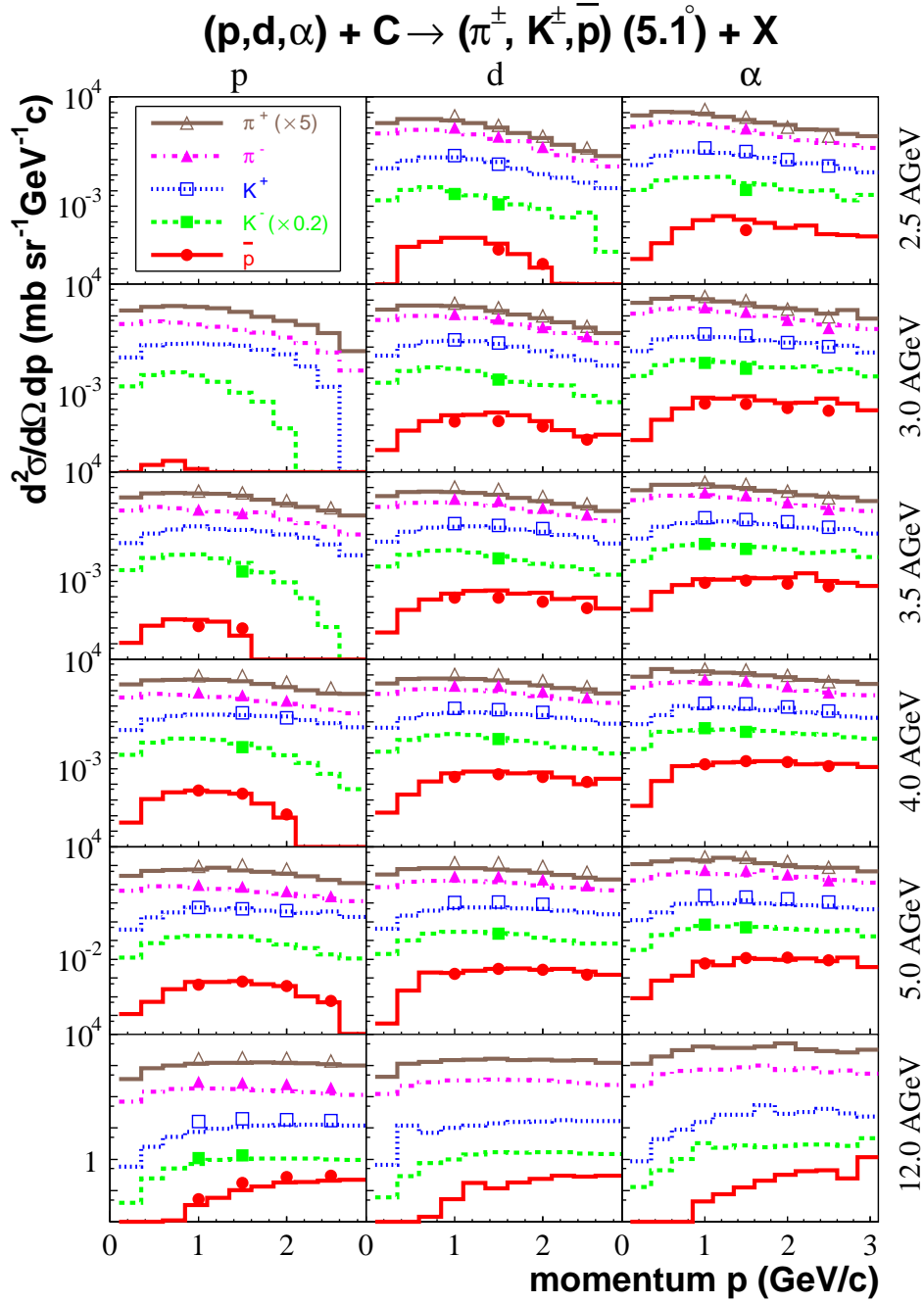


Figure 1. Momentum spectra of π^\pm , K^\pm and \bar{p} [12] (symbols) from pC , dC and αC reactions compared with ROC-model calculations (histograms). Experimental and calculated results for π^+ and K^- mesons are multiplied by the factors indicated in the legend. The scale extends from 10^{-8} to $10^4 \text{ mb sr}^{-1} \text{ GeV}^{-1} \text{ c}$ for energies up to 4.0 A GeV, while the lower limit is 10^{-6} for 5.0 A GeV and $10^{-2} \text{ mb sr}^{-1} \text{ GeV}^{-1} \text{ c}$ for 12.0 A GeV.

from the quarks produced in the first stage of the interaction process. Hadrons are built-up in each FB independently according to the rules of quark statistics [56] by randomly selecting sequences of quarks q and antiquarks \bar{q} . A $q\bar{q}$ gives a meson, while baryons or antibaryons are formed from qqq or $\bar{q}\bar{q}\bar{q}$. From a given sequence of quarks the different hadrons are formed according to the tables of the particle data group [57]. There is no parameter which directly determines the ratio between meson and baryon production as, e.g., in the PYTHIA-LUND model [58–61]. Only an indirect influence via the temperature and the volume parameters is possible, which changes the relative weights of the FBs in dependence on their invariant mass and final particle multiplicity, respectively. (See [30] for a more detailed consideration of hadron formation.)

It is, therefore, remarkable that the general trend of the energy dependence of the data for all projectile types, moderate increase with energy of the cross sections for the light mesons and steep increase of that for the antiprotons, is well described by the calculations. Also the shift of the maximum in the \bar{p} spectra towards higher momenta is reproduced. A similar tendency can be observed if the cross sections from dC and αC reactions are compared to those from pC interactions. The heavier the observed particle the steeper the increase of the cross sections for the heavier projectiles, especially at the lowest incidence energies.

In order to make the presented results more obvious we show in figures 2 and 3 the partial spectra from collisions of a projectile with b target nucleons

$$[a] + [b]$$

for the three projectile types and two selected ejectiles \bar{p} and π^+ . These partial spectra represent incoherent sums over contributions from all possible charge numbers (see (1)) according to

$$d\sigma_{ab}(s) = \sum_{z_a=\max(0, a-\mathcal{N}_A)}^{\min(a, \mathcal{Z}_A)} \sum_{z_b=\max(0, b-\mathcal{N}_B)}^{\min(b, \mathcal{Z}_B)} \sigma_{az_a bz_b} \frac{dW(s; \alpha_{az_a bz_b})}{\sum \alpha_{az_a bz_b} \int dW(s; \alpha_{az_a bz_b})} .$$

The partial spectra result from the interplay between the values of the integrated partial cross sections

$$\sigma_{ab} = \sum_{z_a=\max(0, a-\mathcal{N}_A)}^{\min(a, \mathcal{Z}_A)} \sum_{z_b=\max(0, b-\mathcal{N}_B)}^{\min(b, \mathcal{Z}_B)} \sigma_{az_a bz_b} .$$

and the energy dependence of the relative weights $dW(s; \alpha_{az_a bz_b})$ representing the production cross section in the $[a] + [b]$ interaction. In the case of $p+A$ reactions the σ_{1b} decrease monotonically with increasing number b of participating target nucleons, while for $A+A$ interactions symmetric combinations $a = b$ are preferred. Decisive for subthreshold particle production is the steep increase of the production cross section with the available energy above the threshold in the $[a] + [b]$ interaction under consideration. This explains the small contributions from the $[1] + [1]$ interactions, although σ_{11} represents for all projectile types the largest partial cross section. It is the small available energy which prevents higher \bar{p} production. With increasing number of participants both the mean available energy and the number of competing final channels increase. This results in maximal contributions from the combinations $[1]+[2]$ and $[1]+[3]$ in case of $p+A$ reactions. The spectral distributions are rather independent

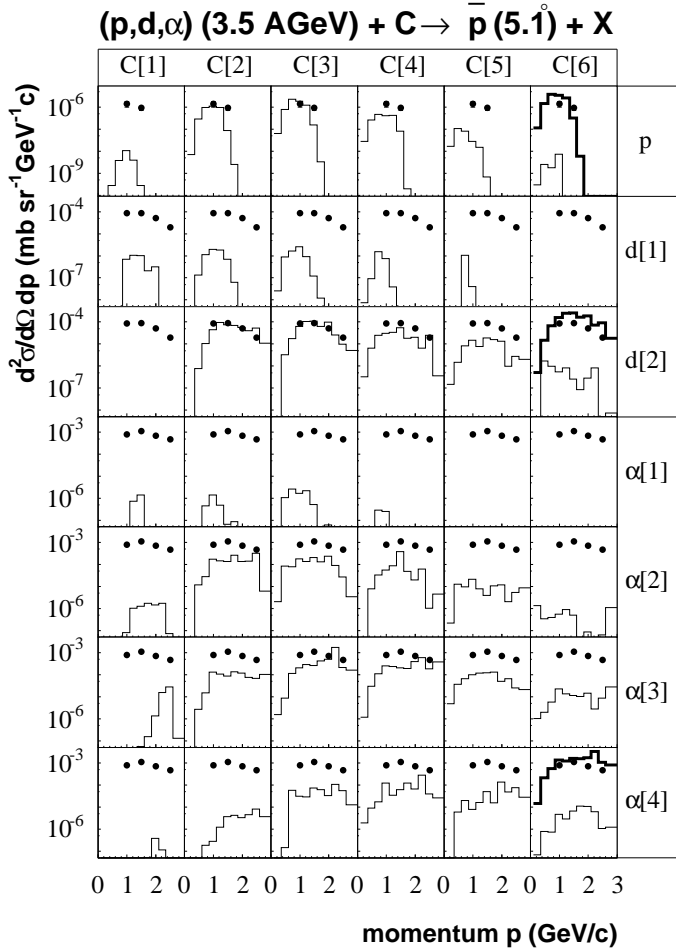


Figure 2. Partial spectra of \bar{p} production calculated for pC , dC and αC reactions (thin histograms) compared to the data [12] (full circles). In six columns denoted by $C[b]$ the spectra from interactions with b participating target nucleons are plotted. Likewise, in the rows the numbers of participants in case of d - and α -induced reactions is denoted by $d[a]$ and $\alpha[a]$, respectively. The thick histograms are the sums of the partial spectra and coincide with the corresponding results from figure 1.

of the number of target participants b , see first row in figure 2. This explains the successful description of the spectra in the ‘first-chance NN collision’ approach, which corresponds to the $[1] + [1]$ process of the ROC model, by appropriately selecting the normalization [12]. Thus, the interpretation of the pC data by the ROC model is quite contradictory to the assumptions of a ‘first-chance NN collision model’. Comparing the $[1] + [1]$ spectra from pC and dC reactions only a moderate increase of \bar{p} production is predicted by the ROC model due to the Fermi motion in the deuteron. The enormous enhancement observed stems mainly from processes with both nucleons of the deuteron and several target nucleons involved where the energy available for particle production

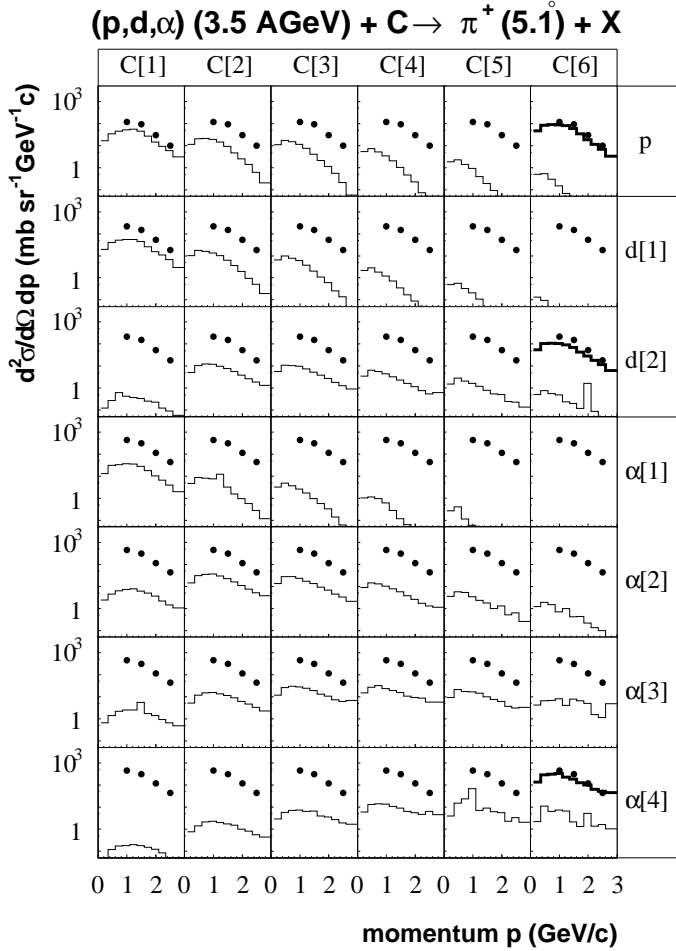


Figure 3. The same as figure 2 for π^+ .

is much larger than in $[1]+[1]$ processes. In case of αC reactions, the number of partial spectra contributing essentially increases. Here the larger available energy arises both from the larger masses of the interacting subsystems and from their internal motion in the projectile and the target. Thus, one can conclude from the viewpoint of the ROC model that the key quantity for understanding subthreshold particle production is the number of participating nucleons. A direct experimental determination of this number for subthreshold \bar{p} production is highly desirable as discussed in [34] for the case of K^- production in pA reactions.

If we consider particle production far above the threshold as in figure 3 then the main difference to subthreshold production consists in the higher value of the energy available for the production of the considered particle. This leads to a smoother energy dependence of the production cross section for the particle under consideration and the gain of available energy due to cluster-cluster processes does not play such an important role. In this way, the partial spectra reflect primarily the values of the

corresponding partial cross sections σ_{ab} with only minor corrections due to the energy dependence of the production cross section. Thus, the $[1] + [1]$ processes with the largest partial cross section for all projectile types yield also the main contributions to the spectra.

4. Summary

Subthreshold particle production is a collective phenomenon which is far from being completely understood. From the viewpoint of the ROC model, data on subthreshold particle production can be reproduced by considering the interaction of few-nucleon groups in complete analogy to the interaction of single nucleons, also with regard to high-momentum transfer processes. It has been demonstrated here that the cluster concept yields a quite natural explanation of the enhancement of subthreshold particle production due to the energy gain in the interaction of few-nucleon groups compared to NN interactions. This concept should be applicable not only in proton- or light-ion-induced reactions, but also for heavy-ion interactions, although in the latter case the number of partial processes increases tremendously. In this sense, the ROC model can be considered as a promising approach to a unified description of particle production processes in a large variety of different types of nuclear reactions.

Acknowledgments

One of the authors (H.M.) would like to thank W. Enghardt for the promotion of this study and A. Sibirtsev for useful discussions.

References

- [1] Chamberlain O, Segré E, Wiegand C and Ypsilantis T 1955 *Phys. Rev.* **100** 947
- [2] Chamberlain O, Chupp W, Goldhaber G *et al.* 1956 *Nuovo Cimento* **3** 447
- [3] Elioff T *et al.* 1962 *Phys. Rev.* **128** 869
- [4] Dorfan D E *et al.* 1965 *Phys. Rev. Lett.* **14** 995
- [5] Baldin A *et al.* 1988 *JETP Lett.* **48** 137
- [6] Caroll J *et al.* 1989 *Phys. Rev. Lett.* **62** 1829
- [7] Shor A *et al.* 1989 *Phys. Rev. Lett.* **63** 2192
- [8] Schröter A *et al.* 1993 *Nucl. Phys. A* **553** 775c
- [9] Schröter A *et al.* 1994 *Z. Phys. A* **350** 101
- [10] Lepikhin Y B, Smirnitsky V A and Sheinkman V A 1987 *JETP Lett.* **46** 275
- [11] Chiba J *et al.* 1993 *Nucl. Phys. A* **553** 771c
- [12] Sugaya Y *et al.* 1998 *Nucl. Phys. A* **634** 115
- [13] Li G Q, Ko C M, Fang X S and Zheng Y M 1994 *Phys. Rev. C* **49** 1139
- [14] Batko G, Cassing W, Mosel U, Niita K and Wolf G 1991 *Phys. Lett. B* **256** 331
- [15] Huang S W, Li G, Maruyama T and Faessler A 1992 *Nucl. Phys. A* **547** 653
- [16] Cassing W, Lang A, Teis S and Weber K 1994 *Nucl. Phys. A* **545** 123c
- [17] Teis S, Cassing W, Maruyama T and Mosel U 1993 *Phys. Lett. B* **319** 47
- [18] Teis S, Cassing W, Maruyama T and Mosel U 1994 *Phys. Rev. C* **50** 388
- [19] Cassing W, Lykasov G and Teis S 1994 *Z. Phys. A* **348** 247
- [20] Batko G, Faessler A, Huang S, Lehmann E and Rajeev K 1994 *J. Phys. G* **20** 461
- [21] Hernández E, Oset E and Weise W 1995 *Z. Phys. A* **351** 99
- [22] Sibirtsev A, Cassing W, Lykasov G I and Rzjanin M V 1998 *Nucl. Phys. A* **632** 131
- [23] Koch P and Dover C B 1989 *Phys. Rev. C* **40** 145
- [24] Ko C M and Ge X 1988 *Phys. Lett. B* **205** 195
- [25] Ko C M and Xia L H 1989 *Phys. Rev. C* **40** R1118
- [26] D'yachenko A T 2000 *J. Phys. G* **26** 861
- [27] Danielewicz P 1990 *Phys. Rev. C* **42** 1564

- [28] Komarov V I, Müller H and Sibirtsev A 2004 *J. Phys. G.* **30** 921.
<http://arXiv.org/nucl-th/0312087>
- [29] Müller H 1995 *Z. Phys. A* **353** 103
- [30] Müller H 2001 *Eur. Phys. J. C* **18** 563. <http://arXiv.org/hep-ph/0011350>
- [31] Müller H and Sistemich K 1992 *Z. Phys. A* **344** 197
- [32] Müller H 1991 *Z. Phys. A* **339** 409
- [33] Müller H 1995 *Z. Phys. A* **353** 237
- [34] Müller H 1996 *Z. Phys. A* **355** 223
- [35] Shmakov S, Uzhinskii V and Zadorozhny A 1988 *Comp. Phys. Communications* **54** 125
- [36] Glauber R J and Mathiae J 1970 *Nucl. Phys. B* **21** 135
- [37] Knoll J 1979 *Phys. Rev. C* **20** 773
- [38] Knoll J 1980 *Nucl. Phys. A* **343** 511
- [39] Bohrmann S and Knoll J 1981 *Nucl. Phys. A* **356** 498
- [40] Shyam R and Knoll J 1984 *Nucl. Phys. A* **426** 606
- [41] Shyam R and Knoll J 1986 *Nucl. Phys. A* **448** 322
- [42] Knoll J and Shyam R 1988 *Nucl. Phys. A* **483** 711
- [43] Ghosh B and Shyam R 1990 *Phys. Lett. B* **234** 248
- [44] Ghosh B 1992 *Phys. Rev. C* **45** R518
- [45] Elton L R 1961 *Nuclear sizes/L. R. B. Elton* (London : Oxford Univ. Pr.)
- [46] Lacombe M *et al.* 1981 *Phys. Lett. B* **101** 139
- [47] Goldhaber A S 1974 *Phys. Lett. B* **53** 306
- [48] Shor A, Perez-Mendez V and Ganezer K 1990 *Nucl. Phys. A* **514** 717
- [49] Geaga J V *et al.* 1980 *Phys. Rev. Lett.* **45** 1993
- [50] Ciofi degli Atti C and Simula S 1996 *Phys. Rev. C* **53** 1689
- [51] Benhar O, Fabrocini A and Fantoni S 1989 *Nucl. Phys. A* **505** 267
- [52] Sick I, Fantoni S, Fabrocini A and Benhar O 1994 *Phys. Lett. B* **323** 267
- [53] Sibirtsev A, Cassing W and Mosel U 1997 *Z. Phys. A* **358** 357
- [54] Byckling E and Kajantie K 1973 *Particle Kinematics* (John Wiley and Sons, London, New York, Sydney, Toronto)
- [55] Westfall G *et al.* 1978 *Phys. Rev.* **C17** 1368
- [56] Anisovich V V and Shekhter V M 1973 *Nucl. Phys. B* **55** 455
- [57] Caso C *et al.* 1998 *Eur. Phys. J. C* **3** 1
- [58] Andersson B, Gustafson G, Ingelman G and Sjostrand T 1983 *Phys. Rep.* **97** 31
- [59] Andersson B, Gustafson G and Nilsson-Almqvist B 1987 *Nucl. Phys. B* **281** 289
- [60] Sjöstrand T and van Zijl M 1987 *Phys. Rev. D* **36** 2019
- [61] Sjöstrand T 1994 *Comput. Phys. Commun.* **82** 74